

# MAGNETIC FIELD OF THE 40–80 MeV H<sup>-</sup> ISOCHRONOUS CYCLOTRON AT GATCHINA. EXPERIMENTS AND 3D CALCULATIONS

S.A. Artamonov, D.A. Amerkanov, G.I. Gorkin, V.P. Gres, E.M. Ivanov, G.A. Riabov

## 1. Introduction

The isochronous cyclotron C-80 which is now started up at the PNPI is planned to be used as for applied physics program – for production of medicine isotopes, for therapy of eye melanoma and surface forms of cancer, for radiation resistance tests of electronic components – as well as for fundamental research in nuclear physics, solid state physics and biology. Here we present the final parameters of the magnetic field distribution of the new H<sup>-</sup> isochronous cyclotron and results of 3D computer calculations and experimental measurements.

The magnet and the magnetic system are the most important and expensive parts of the cyclotron, and a considerable attention was paid to their design. The magnetic field of the cyclotron C-80 should meet several requirements. The magnetic field rigidity at the final orbit must reach  $Br = 13.2$  kGs · m, which corresponds to 80-MeV energy of the proton beam. For insuring the isochronism, the magnetic field averaged over the azimuth when going from the centre of the magnet to the final orbit should increase by ~8.5%. The azimuthal variation of the magnetic field should provide the vertical and horizontal transversal focusing. Some room should be left for a high frequency system: the gap between the shims should be wider than 160 mm. In distinction from a standard cyclotron, there is an additional and essential requirement for an H<sup>-</sup> machine – to keep H<sup>-</sup> losses due to dissociation less than some percent. Acceleration of H<sup>-</sup> ions has obvious advantages: a possibility for 100 % extraction of the beam with high intensity and variable energy. On the other hand, it requires a special source of H<sup>-</sup> ions, high vacuum, and what is most important, the magnetic field strength in the magnet sector should not exceed in our case 16.8 kGs to prevent H<sup>-</sup> electromagnetic dissociation.

## 2. General description

A few years ago, as a first approximation, the magnetic structure of the cyclotron was designed on the basis of 2D calculations by using the POISSON program and measurements on two small models [1, 2]. The geometry and the key parameters of the magnetic system for the cyclotron were selected. It was supposed that the height of each of the sectors would be equal to 90 mm, and during further optimization it was not changed. For obtaining the required isochronism, the height of the correction sector shims was varied. The initial height of these shims was selected equal to 20 mm. Besides, in the course of the optimization, a special constrained condition was imposed. It was required that the amplitude of the main fourth field harmonic should not exceed ~3 000 Gs, and the field near the extraction radius  $r \approx 90$  cm should be  $B \leq 16 800$  Gs. To reduce H<sup>-</sup> dissociation losses, a magnetic structure of C-80 with high spiral angles was proposed. Under these conditions, the H<sup>-</sup> dissociation should be below 5% [3]. For these purposes, additional valley shims were introduced into the magnetic system, and their geometrical parameters were also varied. Thus, the formation of the demanded isochronous field was carried out only by changing the iron shims geometry without using correction coils. For an improvement of the accelerated beam orbits centering and reducing lower magnetic field harmonics (1, 2, 3), four pairs of azimuthal correcting coils were installed between the sectors at the radii 85–1 025 mm.

The extraction of the beam of variable energy 40–80 MeV in the H<sup>-</sup> isochronous C-80 cyclotron is performed without variation of the magnetic field but by changing the radial position of the stripping foil.

The major unit of the cyclotron, its electromagnet, was designed using the model of the magnet of the PNPI SC-1000 synchrocyclotron (SP-72). This electromagnet has a traditional design with an E-shaped magnet yoke and a pole of 2.05 m in diameter. The system to move upward the magnet upper part (the half-yoke) was worn-out and outdated. Therefore, it was replaced with four pairs of ball bearings and screws equipped with servomechanisms and position sensors. The maximum height of the half-yoke lifting is about 600 mm, the setting accuracy is better than 50 μm.

Main parameters of the C-80 magnetic structure are presented in Table.

**Table**

Main magnet parameters

Parameter	Value
Pole diameter	2.05 m
Valley gap	386 mm
Hill gap (min)	163 mm
Number of sectors	4
Spiral angle (max)	65°
Field in the centre	1.352 T
Flutter (max)	0.025
Ampere-turns	$3.4 \cdot 10^5$
Power	120 kW
Weight	250 t

### 3. 3D optimization

The main parameters of the cyclotron magnetic system were refined and optimized by computer simulations with the 3D MERMAID code [4, 5], and the dynamics simulations were performed with the code in Ref. [6]. The main peculiarities and modifications of the preliminary design can be formulated as follows.

The detailed 3D geometry of the magnet yoke, of the sectors (four pairs), sector shims (17 correction shims in each sector), and the valley shims, the coils, and the external boundaries was introduced in the computer model. Because of a big angular extension of the spiral sectors in C-80, it was necessary to use in the calculations a half of the magnet with the corresponding symmetry boundary conditions. The external boundary of the area where the calculations were performed was chosen rather far to get rid of its influence on the magnetic field in the working region and to determine correctly the fringe field. The fringe field was taken into account for correct calculations of the extraction beam optics. Thus, for the description of the magnetic structure of C-80 using the MERMAID program, about 20.5 million direct prisms were required, which allowed to reach the necessary precision of  $10^{-3}$ – $10^{-4}$  in the calculations of the magnetic field.

The nonlinear magnetic properties of the used electro technical steels (three types) were taken into account. To increase the vertical focusing in the central region, the zero and low spiral sectors were prolonged from the radius of 27 cm to the radius of 40 cm.

In the preliminary version of the magnet structure, four valley shims in each valley were used to provide isochronisms on the last radii. To cut down the number of the valley shims from four to one, the azimuthal width of the sectors was expanded by  $\sim 20$  mm from the radius of 70 cm to the final radius of 102.5 cm. Under these conditions, the  $H^-$  dissociation is below 3 % [5].

Only the 3D field calculations made possible to perform the central region design taking into account the axial injection system geometry and the design of the magnetic field bump for the beam focusing at the first turns.

### 4. Main results

At the final stage of the magnetic field formation, the computer calculations and the magnetic field measurements were performed in parallel. The magnetic field in the full scale magnet was measured using a system based on twenty nuclear magnetic resonance calibrated Hall probes and an automated coordinate system, which could position probes in the cylindrical coordinate system with an accuracy of 0.1 mm along the radius at each azimuthal angle (with steps 0.5, 1, 1.5, 2, or 2.5°) at the radii from zero up to 100 cm (with steps 0.5, 1, 1.5, 2, or 2.5 cm). The total measurement accuracy was about 0.02%. The time of the magnet

topography measurements on the super period was ~ 6–8 h and on the periodicity element was about 2 h. The local field defects were corrected by using iron shims. The necessary shim thickness was estimated by 3D calculations. Disagreements between the computer predicted and the measured fields did not exceed some Gs.

The final field distribution (Fig. 1) was reached by selection of the thickness of the 17 types of the iron sector shims in every sector and selection of the thickness of the valley shims by using the trial-and-error method.

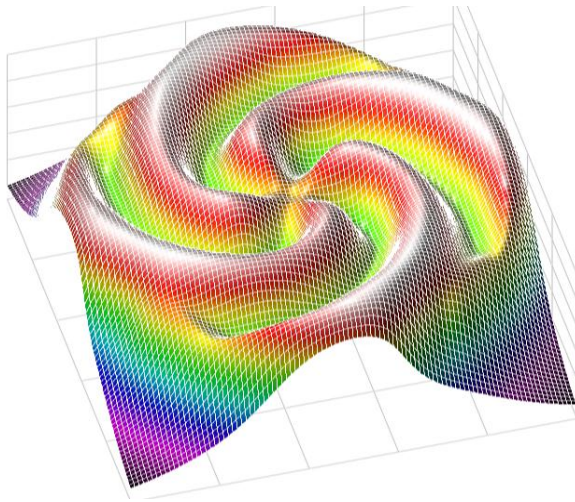


**Fig. 1.** Final magnetic field distribution

As a result, the magnetic field was obtained which provided the beam acceleration from the radius of ~ 15 mm up to the radius of ~ 90 cm.

We remind that in the working magnet gap four pairs of sectors with high spirality angles were placed. Coils for the correction of the average magnetic field were not used in the cyclotron C-80. For improvement of the accelerated beam orbits centering, four pairs of azimuthal correcting coils between the sectors were installed at the radii 85–1 025 mm.

The comparison of the measured average magnetic field and its isochronous value is shown in Fig. 2.

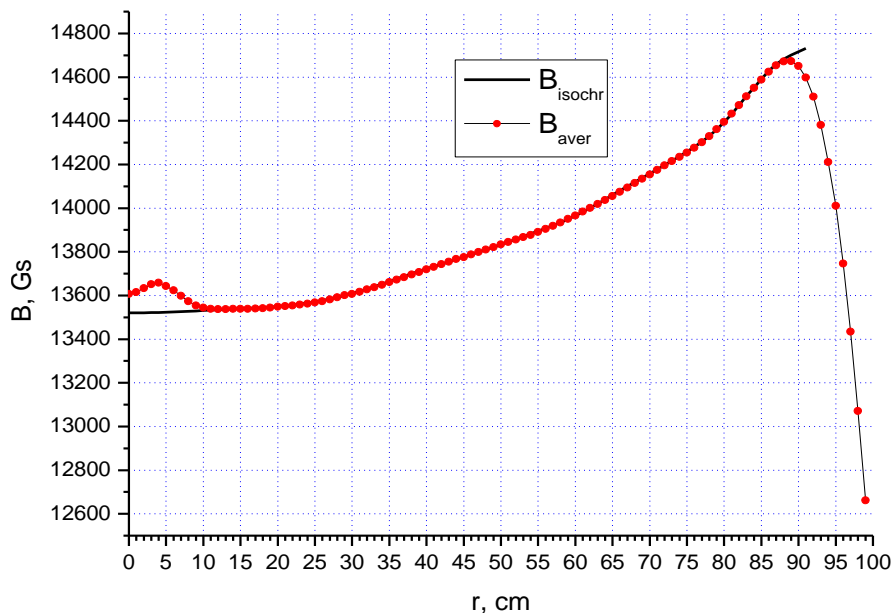


**Fig. 2.** Comparison of the measured magnetic field  $B_{\text{aver}}$  and the isochronous field  $B_{\text{isochr}}$

The isochronism of the magnetic field was provided with the accuracy of 2–5 Gs. The difference between the measured magnetic field and the isochronous cyclotron field is presented in Fig. 3.

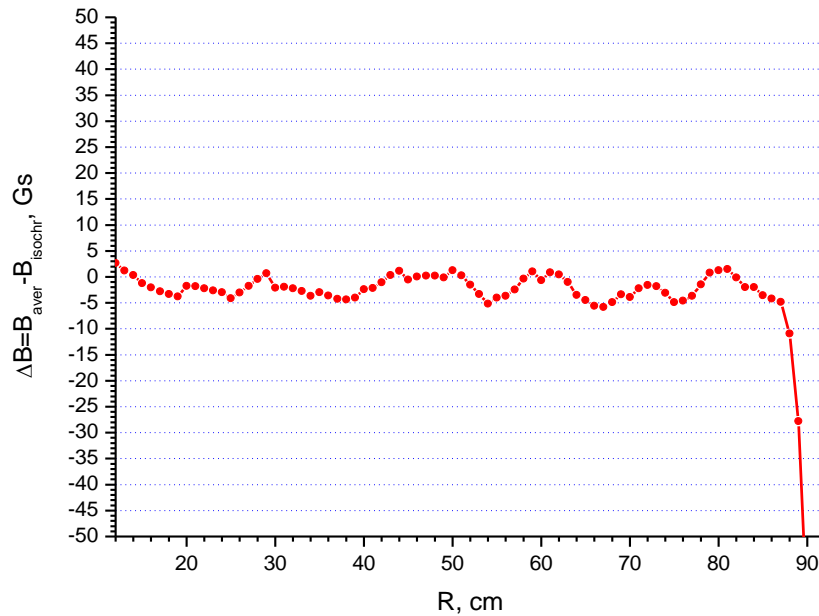


**Fig. 3.** Difference between the measured magnetic field and the isochronous cyclotron field

The measured harmonics of the magnetic field versus the radius are shown in Fig. 4. It is seen that at the interface of the direct sector with its spiral part, there is a significant decrease of the main harmonic  $A_4$ . Near the extraction radii, a growth of the harmonic  $A_{12}$  is observed, which hinders the drop of the harmonic  $A_4$ .

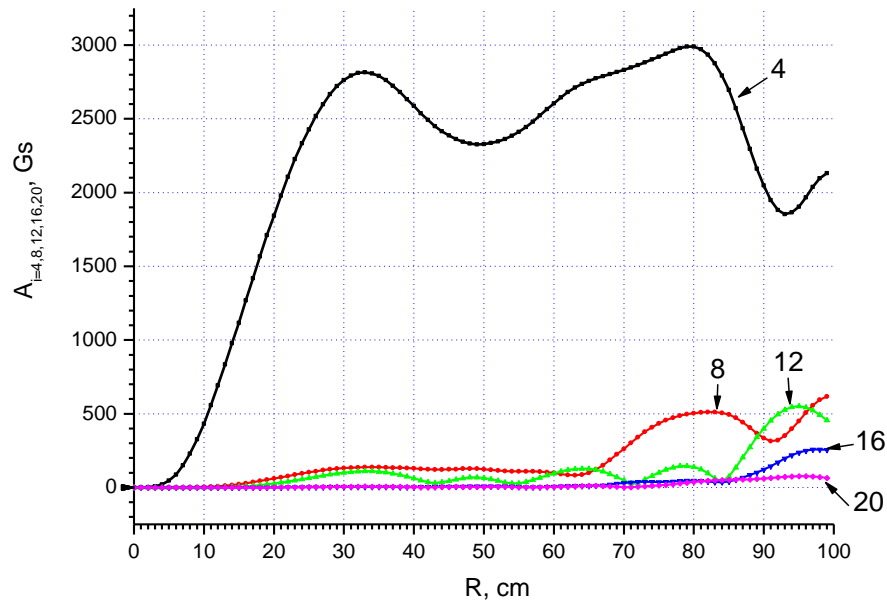


**Fig. 4.** Measured harmonics (4, 8, 12, 16, and 20) of the magnetic field versus the radius

A special attention was paid to reduce the lower harmonics (Fig. 5). The most dangerous harmonics  $A_1$ ,  $A_2$ ,  $A_3$  lead to strong distortions of the accelerated orbits. After considerable efforts in our case, the first harmonic on the last radii did not exceed 10–12 Gs.

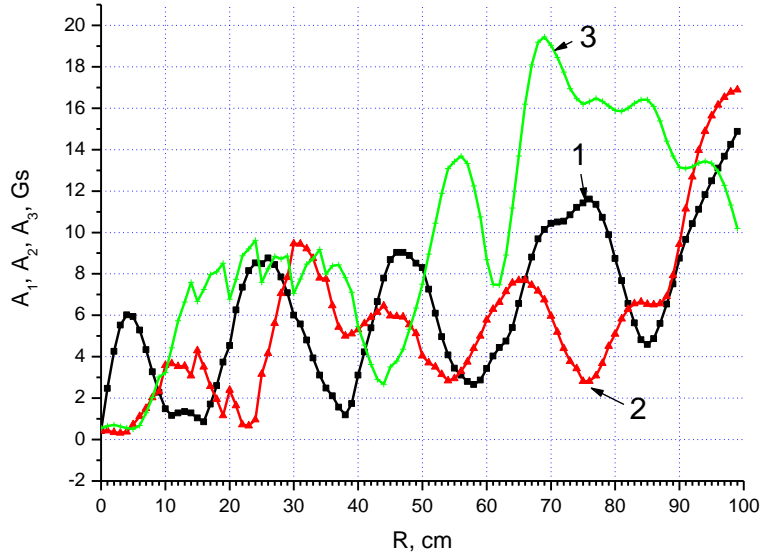


**Fig. 5.** Measured lower harmonics of the magnetic field versus the radius

The first and second harmonics of the magnetic field perturbations have an essential influence on the radial motion of the beam in C-80. The amplitude of the first harmonic is determined by inaccuracies in production and assembling of the cyclotron magnet. The amplitude of the second harmonic at the last radii is less than 8 Gs.

The nature of the action of these harmonics on the beam dynamics is various. The amplitude of the first harmonic noticeably affects the coherent radial oscillations of the beam, since betatron frequency  $\nu_r$  in the entire acceleration region is close to 1.

The gradient of the increase of the amplitude of the second harmonic is the driving term of the parametric resonance  $2\nu_r = 2$ . In principle, this resonance can lead to an increase of free radial incoherent oscillations of the ions and also to a growth of the radial emittance. The effective force of this resonance depends on specific conditions: the value of the gradient, how far the working point is located from the resonance, and the duration of the resonance action.

The first, second, and third harmonics can be compensated only by harmonic coils. In the every valley A, B, C, and D there are four types of the correction coils I, II, III, IV (Fig. 6). The magnetic fields of these four harmonic coils was measured and examined. These coils are used to decrease the lower harmonics  $A_1, A_2, A_3$  of the cyclotron magnetic field. The contributions of the harmonic coils magnetic fields into the measured average field of the cyclotron are presented in Fig. 7.

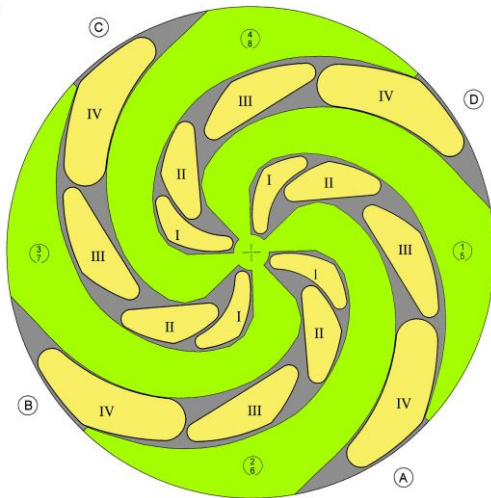


**Fig. 6.** Top view of the pole tip of C-80

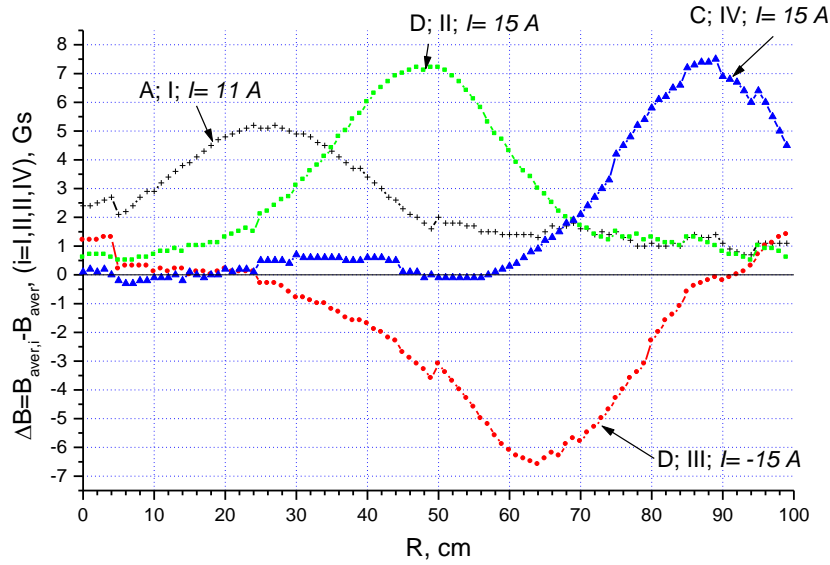


**Fig. 7.** Contributions of the harmonic coil magnetic fields into the measured average field of the cyclotron

The nominal currents in the harmonic coils were selected as follows: I –  $I = \pm 25$  A, II –  $I = \pm 25$  A, III –  $I = \pm 25$  A, IV –  $I = \pm 42$  A.

The measured magnetic field allows the vertical and horizontal focusing (Fig. 8) and the isochronism in the acceleration region [7].

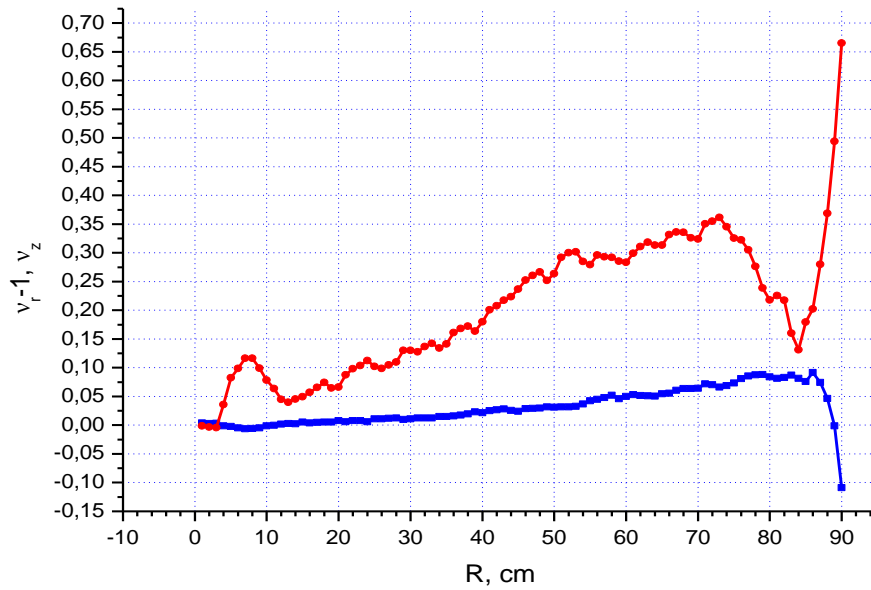


**Fig. 8.** Frequency of free oscillations  $v_r$  (blue) and  $v_z$  (red) versus the average radius of the orbit

A special attention was paid to avoid dangerous resonances. Detailed dynamics simulations were performed to be sure that the resonances which are crossed during the acceleration do not cause a significant harmful effect on the beam. The number of ion turns in C-80 is expected to be about 400.

## 5. Conclusion

Results of the final magnetic field distribution of the 80 MeV  $H^-$  isochronous cyclotron at Gatchina are presented. Main features and problems are connected with applying the high spirality magnetic structure for acceleration of  $H^-$  ions. The formed structure permits to accelerate  $H^-$  ions up to an energy 80 MeV using a rather small two-meter magnet, the beam losses due to the ion dissociation being less than 3%. As far as  $H^-$  cyclotron operates at the fixed magnetic field, the necessary field distribution was obtained by using iron correction shims only. To obtain the necessary field distribution, 3D-computer calculations and successive magnetic measurements were very helpful.

At the present time, all cyclotron systems are installed and tested. In June 2016, a physical start-up of the C-80 cyclotron system was realized. Works were carried out in the pulse mode at low currents of the accelerated beam to exclude strong activation of the equipment to make possible a safe continuation of works in the cyclotron vacuum chamber, with the components of the beam transport system, *etc.* The design parameters of the cyclotron were obtained in November 2016.

## References

1. N.K. Abrossimov, S.A. Artamonov, V.A. Eliseev, G.A. Riabov, in *Proc. of the Second Int. Workshop: Beam Dynamics & Optimization – BDO, St. Petersburg, 1995*, pp. 7–15.
2. N.K. Abrossimov, S.A. Artamonov, V.A. Eliseev, G.A. Riabov, in *Proc. of the XV Int. Conf. on Cyclotron and Their Application, Caen, France, 1998*, pp. 518–521.
3. N.K. Abrossimov, S.A. Artamonov, V.A. Eliseev, G.A. Riabov, *PNPI Research Report 1994–1995*, Gatchina, 1996, pp. 275–278.
4. S.N. Andrianov, S.A. Artamonov, A.N. Dubrovin, V.A. Eliseev, *Vestnik SPbSU*, Ser. **10**, Iss. 3, 12 (2008).
5. S.A. Artamonov, E.M. Ivanov, G.A. Riabov, N.A. Chernov. in *Proc. of RuPAC 2012, St. Petersburg, 2012*, WEPPC015, pp. 475–477.
6. S.N. Andrianov, S.A. Artamonov, *Vestnik SPbSU*, Ser. **10**, Iss. 2, 3 (2009).
7. S.A. Artamonov *et al.*, in *Proc. of XX Int. Conf. Beam Dynamics & Optimization, BDO-2014, St. Petersburg, 2014*, pp. 18–19.